nature astronomy

LETTERS

https://doi.org/10.1038/s41550-019-0977-7

Sensitive probing of exoplanetary oxygen via mid-infrared collisional absorption

Thomas J. Fauchez[1,2,3*], Geronimo L. Villanueva[1,3], Edward W. Schwieterman[4,5,6,7,8], Martin Turbet[9], Giada Arney[1,3,7], Daria Pidhorodetska[1,10], Ravi K. Kopparapu[1,3,7], Avi Mandell[1,3] and Shawn D. Domagal-Goldman[1,3,7]

The collision-induced fundamental vibration–rotation band at 6.4 µm is the strongest absorption feature from O_2 in the infrared[1–3], yet it has not been previously incorporated into exoplanet spectral analyses for several reasons. Either collision-induced absorptions (CIAs) were not included or incomplete/obsolete CIA databases were used. Also, the current version of HITRAN does not include CIAs at 6.4 µm with other collision partners (O_2–X). We include O_2–X CIA features in our transmission spectroscopy simulations by parameterizing the 6.4-µm O_2–N_2 CIA based on ref. [3] and the O_2–CO_2 CIA based on ref. [4]. Here we report that the O_2–X CIA may be the most detectable O_2 feature for transit observations. For a potential TRAPPIST-1 e analogue system within 5 pc of the Sun, it could be the only O_2 signature detectable with the James Webb Space Telescope (JWST) (using MIRI LRS (Mid-Infrared Instrument low-resolution spectrometer)) for a modern Earth-like cloudy atmosphere with biological quantities of O_2. Also, we show that the 6.4-µm O_2–X CIA would be prominent for O_2-rich desiccated atmospheres[5] and could be detectable with JWST in just a few transits. For systems beyond 5 pc, this feature could therefore be a powerful discriminator of uninhabited planets with non-biological 'false-positive' O_2 in their atmospheres, as they would only be detectable at these higher O_2 pressures.

We study the strength of the O_2–X collision-induced absorption (CIA) spectral signatures in exoplanets by computing synthetic spectra for various Earth-like atmospheres with the Planetary Spectrum Generator (PSG)[6]. The atmospheres are created with the LMD-G[7] general circulation model coupled with the Atmos[8] photochemical model (see Methods for details). We focus in particular on planets around M dwarfs such as TRAPPIST-1 e. In fact, for modern Earth atmospheric conditions, the 6.4-µm region is overlapped by a wide H_2O absorption band. However, for a modern Earth-like atmosphere on a tidally locked planet in the habitable zone (HZ) of an M dwarf, the terminator region is predicted to be fairly dry (Supplementary Fig. 2). Also, water is mostly confined in a small portion of the atmosphere near the surface, which is under the refraction limit and hidden by clouds (as on Earth, where the troposphere is wet and the stratosphere is dry). Near the top of the atmosphere, H_2O is highly photodissociated (Supplementary Fig. 2). The H_2O signature in the transmission spectra of a habitable planet is therefore expected to be very weak[9,10]. While some trace gases such as NO_2 and N_2O also produce opacity in this spectral region, their concentrations are predicted to be orders of magnitude lower than those that would generate confounding impacts on the simulated spectra.

The TRAPPIST-1 system[11], consisting of seven Earth-sized planets orbiting an ultracool dwarf star, will be a favourite target for atmospheric characterization with the James Webb Space Telescope (JWST) due to its relative proximity to the Earth and the depth and frequency of its planetary transits. Therefore, we use TRAPPIST-1 e as a case study for our simulated spectra. We employed the LMD-G[7] general circulation model and the Atmos photochemical model[8] to simulate TRAPPIST-1 e with boundary conditions similar to those of modern Earth[9]. Figure 1 shows TRAPPIST-1 e transmission spectra from 0.6 to 10 µm for various Earth-like atmospheres simulated with the PSG[6]. Figure 1a shows the impact of cloud coverage on spectral features: clouds diminish the strength of all absorption features, but impact the strength of the O_2–X feature much less strongly than they impact shorter-wavelength O_2 features such as the O_2 A band or the 1.06- and 1.27-µm O_2 CIA used in ref. [12] (which considered only clear-sky atmospheres). This is because water-cloud opacity is stronger at short wavelengths. Figure 1b compares the strength of the O_2–X CIA band with that of the overlapping H_2O absorption band near 6.4 µm for a cloudy atmosphere. O_2–X CIA strongly dominates the absorption in this wavelength range. Figure 1c shows how the strengths of O_2-monomer and CIA absorption features scale as a function of the O_2 atmospheric abundance for O_2 levels ranging from 0.1 times the present atmospheric level of O_2 (PAL) to 2 times PAL. Our results show that the 6.4-µm CIA feature appears to be about three times stronger than the 1.27-µm O_2 CIA feature, and is therefore the strongest O_2 signature across the visible/near-infrared/mid-infrared (VIS/NIR/MIR) spectrum.

Figure 2 shows the number of TRAPPIST-1 e transits needed to detect the O_2 A band, the O_2–O_2 CIA feature at 1.27 µm and the O_2–X CIA feature at 6.4 µm at a 5σ confidence level with JWST for a modern Earth-like cloudy atmosphere on TRAPPIST-1 e orbiting a TRAPPIST-1-like star at distances from Earth ranging from TRAPPIST-1's true distance (12.1 pc) to 2 pc. We can see that the 6.4-µm O_2–X CIA feature requires an order of magnitude fewer transits than the two other O_2 features because of the stronger intrinsic O_2–X CIA absorption at 6.4 µm and because cloud opacity is stronger at shorter VIS/NIR wavelengths. The horizontal dashed

[1]NASA Goddard Space Flight Center, Greenbelt, MD, USA. [2]Goddard Earth Sciences Technology and Research (GESTAR), Universities Space Research Association, Columbia, MD, USA. [3]GSFC Sellers Exoplanet Environments Collaboration, Greenbelt, MD, USA. [4]Department of Earth and Planetary Sciences, University of California, Riverside, CA, USA. [5]NASA Postdoctoral Program, Universities Space Research Association, Columbia, MD, USA. [6]NASA Astrobiology Institute, Alternative Earths Team, Riverside, CA, USA. [7]Nexus for Exoplanet System Science (NExSS) Virtual Planetary Laboratory, Seattle, WA, USA. [8]Blue Marble Space Institute of Science, Seattle, WA, USA. [9]Observatoire Astronomique de l'Université de Genève, 51 chemin de Pégase, Sauverny 1290, Switzerland. [10]University of Maryland Baltimore County/CRESST II, Baltimore, MD, USA. *e-mail: thomas.j.fauchez@nasa.gov

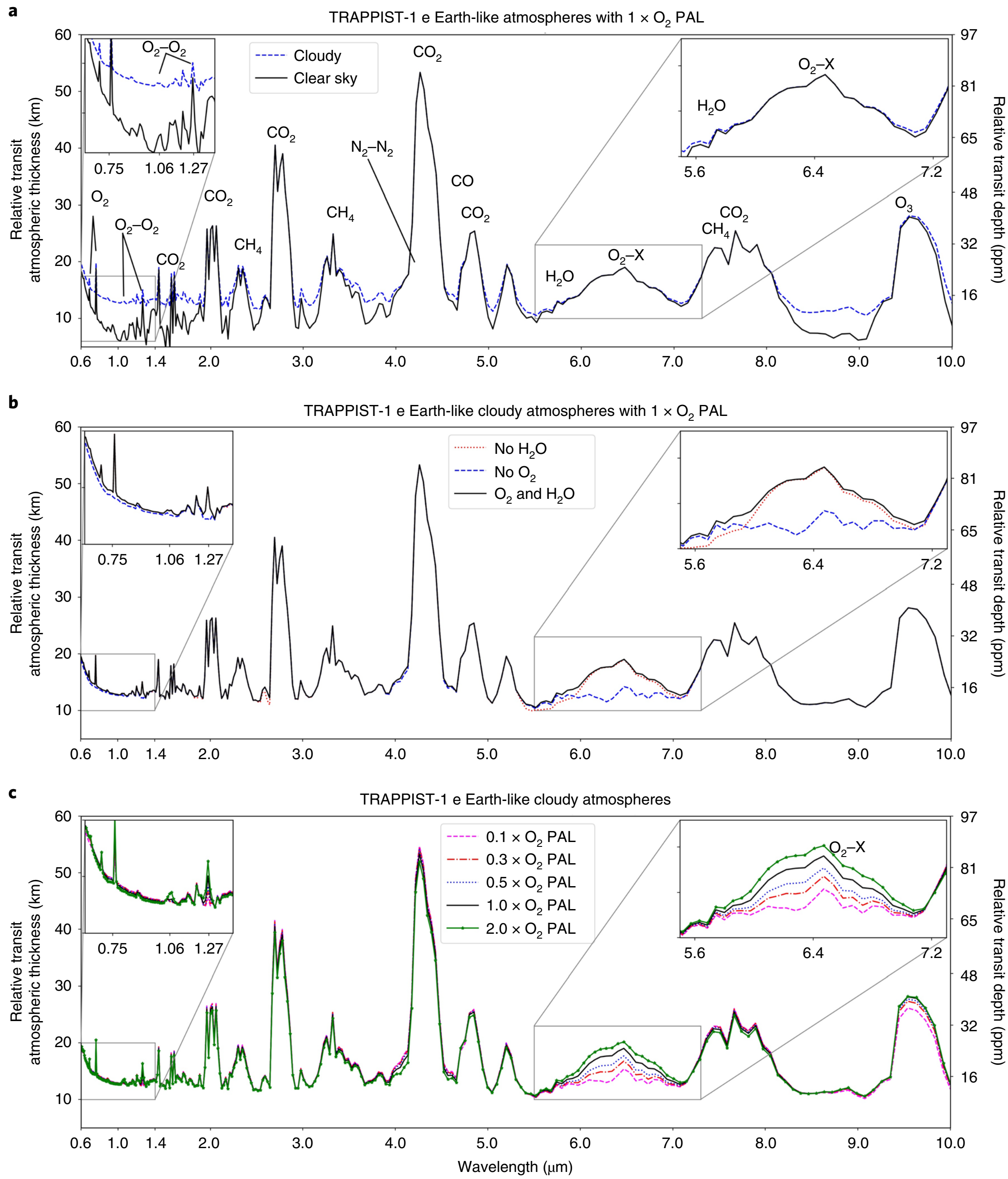

Fig. 1 | Earth-like transmission spectra of TRAPPIST-1 e. **a**, The impact of cloud coverage on the atmosphere's spectral features. **b**, A comparison of the strengths of the O_2–X CIA feature and the H_2O absorption band around 6.4 μm for a cloudy atmosphere. **c**, The strength of O_2-monomer absorptions and CIA features as a function of the amount of O_2 in the atmosphere relative to PAL for a spectrum with clouds included. The O_2–X CIA could be the strongest O_2 feature across the VIS/NIR/MIR spectrum.

red line represents the 85 transits that will occur for TRAPPIST-1 e during the 5-yr nominal lifetime of JWST, thus setting an upper limit on the number of transits observable. Because TRAPPIST-1 e orbits a very small M8 star, it offers one of the best signal-to-noise ratios (SNRs) a habitable planet can have and therefore represents a best-case scenario in terms of detectability. However, even in this context, none of the O_2 features are detectable at 5σ at the distance of the TRAPPIST-1 system. However, the 6.4-μm O_2–X CIA feature could be detectable at 5σ for an analogue system at a star–Earth distance less than 5 pc. Therefore, this simulation shows that the 6.4-μm O_2–X CIA could be the only oxygen feature detectable with JWST for a cloudy modern Earth-like atmosphere for nearby hypothetical TRAPPIST-1 analogue systems. The O_2–X feature for oxygen could also potentially be used to detect non-habitable conditions, such as a desiccated atmosphere rich in bars of abiotic O_2 generated from massive ocean loss[5,10,13–16]. Reference [9] has shown that, for an assumed original water content of 20 Earth oceans (by mass), the TRAPPIST-1 e, f and g planets may have lost between 3 and 6 Earth oceans, resulting in atmospheres with 22 and 5,000 bar of O_2.

Figure 3 shows transit spectra for TRAPPIST-1 e assuming conservative 1-bar O_2-only desiccated and isothermal atmospheres ranging from 200 to 600 K. Relative transit depth (ppm, left-hand

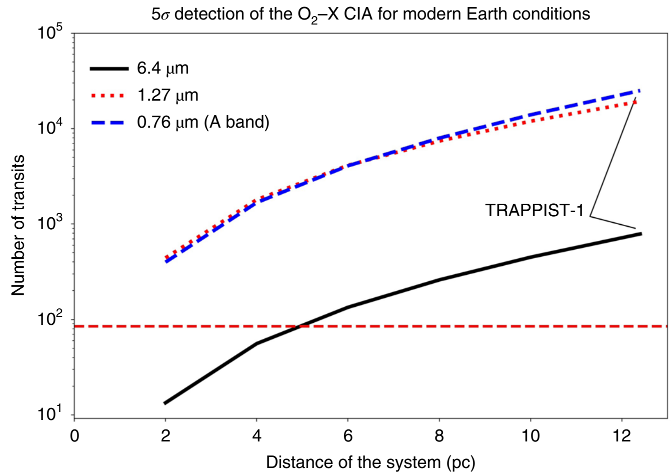

Fig. 2 | Number of TRAPPIST-1 e transits needed for a 5σ detection of the O_2 A band (R = 100), the O_2–O_2 CIA at 1.27 µm (R = 100) and the O_2–X CIA at 6.4 µm (R = 30) with JWST for the TRAPPIST-1 system moved from its distance from the Sun (12.1 pc) to 2 pc. The atmosphere is composed of N_2, 10,000 ppm of CO_2, 10 ppm of CH_4 and 21% O_2 with a surface pressure of 1 bar. Resolving power (R) has been optimized for each band to maximize the SNR. The horizontal dashed red line corresponds to the number of times that TRAPPIST-1 e will be observable transiting in front of TRAPPIST-1 during JWST's 5-yr lifetime (85 transits). The 6.4-µm O_2–X CIA requires far fewer transits than the O_2 A band and the 1.27-µm O_2–O_2 CIA and can be detectable at 5σ for a TRAPPIST-1–TRAPPIST-1 e analogue system closer than 5 pc.

y axis) is the transit depth produced by the atmosphere itself, which can be converted into relative transit atmospheric thickness (km, right-hand *y* axis). These isothermal profiles allow us to test the sensitivity of oxygen spectral features to atmospheric temperature. The atmospheric scale height increases with temperature, and the largest features are seen for the highest temperatures. Note that O_2–O_2 CIA opacities in HITRAN are only provided in the 193–353-K temperature range. Therefore, for the isothermal profiles beyond 353 K we used the 353-K CIA coefficients. We can see that the 6.4-µm O_2–O_2 CIA feature is broad (~3 µm) and strong (40–90 ppm). The 1.27-µm O_2–O_2 CIA feature reaches a similar relative transit depth but is narrower (widths of ~0.2 µm). In addition, the continuum level for the shorter wavelengths is raised by the Rayleigh scattering slope, reducing the NIR CIA relative transit depths to 50–80 ppm, respectively. Similarly, the O_2 A band reaches very large transit depths (up to 110 ppm) but on a high continuum, which reduces its relative strength to 95 ppm. The larger width of the O_2–X CIA feature at 6.4 µm allows us to bin the data to a lower resolving power, improving the SNR and therefore compensating for a higher noise floor in the MIRI LRS (Mid-Infrared Instrument low-resolution spectrometer) range. Supplementary Table 1 presents the relative transit depth, one-transit SNR and number of transits for 3σ and 5σ detections for TRAPPIST-1 e assuming a 1- and 22-bar desiccated atmosphere on TRAPPIST-1 e, and Supplementary Fig. 3 is similar to Fig. 2 but for the 22-bar O_2 desiccated and isothermal atmospheres.

Interpreting an O_2 detection via the O_2–O_2 CIA band at 6.4 µm will be strengthened by constraining the concentration of O_2, and placing its presence in a broader atmospheric context. For HZ planets with a planet–star contrast comparable to that of TRAPPIST-1 e and within 5 pc of the Sun, next-generation MIR observatories could detect O_2 at concentrations similar to that of modern Earth using the 6.4-µm O_2–X feature. In combination with detections of other MIR features from CH_4, H_2O or N_2O, this would represent a strong biosignature with no known non-biological explanations[17]. Note that there are 50 red dwarfs within 5 pc of the Sun (http://www.recons.org/TOP100.posted.htm). For systems farther than about 5 pc and/or HZ planets orbiting earlier M dwarfs, JWST or future MIR observatories may be able to detect the 6.4-µm O_2–X feature only for O_2 concentrations orders of magnitude higher than those

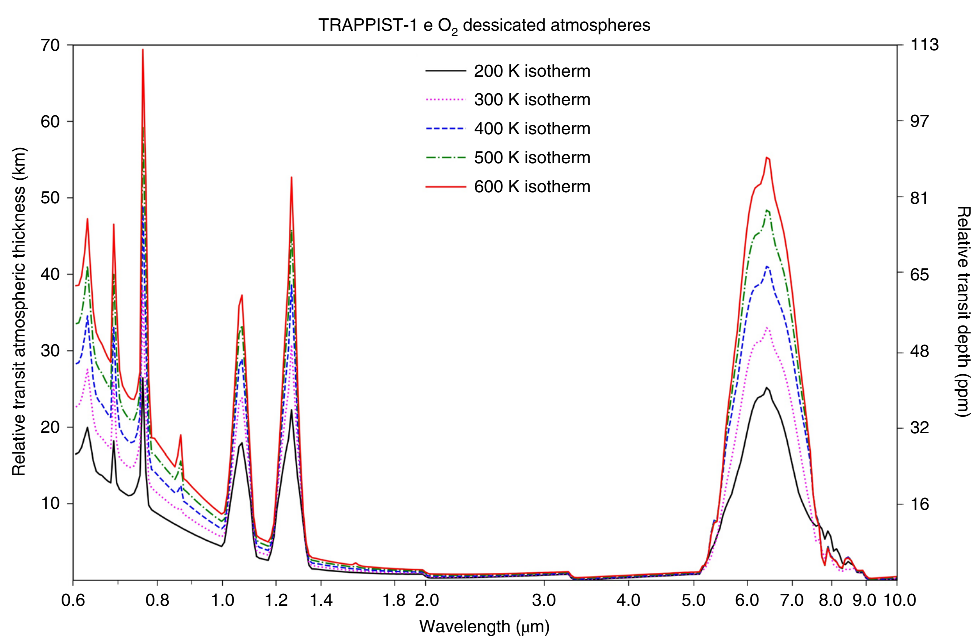

Fig. 3 | Transmission spectra for a 1-bar O_2 desiccated atmosphere on TRAPPIST-1 e assuming various isothermal profiles. Depending on the temperature, the 6.4-µm O_2–O_2 CIA feature can reach between 40 and 90 ppm, which is comparable to or larger than the O_2 A-band and 1.06- and 1.27-µm O_2 CIA features. No photochemistry is considered here so O_3 is missing from the spectra. Note that the increase of the relative transit atmospheric thickness and relative transit depth is due to the increase of the scale height with temperature.

on modern-day Earth, which would be indicative of a desiccated, O_2-rich, uninhabitable planet.

Detection of this feature for planets within the HZ[18–20] will test the hypothesis that the high-luminosity pre-main-sequence-phase M dwarfs endure can render even current HZ planets uninhabitable[5]. Finally, detection of this feature would answer the question of whether planets around M dwarfs can sustain an atmosphere.

Methods

Parameters for TRAPPIST-1 e. In this study, the TRAPPIST-1 e planet's parameters have been set up from refs. [11,21]. The TRAPPIST-1 spectrum of ref. [9] has been used for our photochemical simulations with the Atmos model.

Monomer and CIA pressure sensitivity. Monomer and CIA optical depths can be expressed by the following equations[12]:

$$d\tau_{\rm mono} = \sigma\rho\, dl = \sigma P/T\, dl \tag{1}$$

$$d\tau_{\rm CIA} = k\rho^2\, dl = k(P/T)^2\, dl \tag{2}$$

with $d\tau_{\rm mono}$ and $d\tau_{\rm CIA}$ representing the monomer and CIA differential optical depths, respectively; σ and k are the monomer and CIA cross-sections, respectively; ρ is the number density of the gas; P is the pressure; T is the temperature and dl is the path length. $d\tau_{\rm mono}$ is proportional to P and $d\tau_{\rm CIA}$ to P^2, and this difference of sensitivity may be used to estimate the atmospheric pressure[12].

Atmospheric modelling. We use the Atmos[8] photochemical model to self-consistently simulate Earth-like atmospheres with a variety of O_2 partial pressures on TRAPPIST-1 e. The terminator temperature, gas mixing ratio, vapour and condensed-water (liquid and ice) profiles have been provided from the LMD-G[7] global climate model simulations of a 1-bar TRAPPIST-1 e modern Earth atmosphere. In Atmos, some of the N_2 has been swapped for O_2 to obtain various O_2 PAL values as shown in Fig. 1, both gases having no greenhouse effect except through pressure broadening or CIA, and 10,000 ppm of CO_2 and 10 ppm of CH_4 have been assumed. Due to the terminator atmospheric profiles varying with latitude, Atmos was used to calculate profiles for 98 latitude points, determined by the LMD-G latitude resolution.

Transmission spectrum simulations. PSG[6] has been used to simulate JWST transmission spectra. PSG is an online radiative-transfer code that is able to compute planetary spectra (atmospheres and surfaces) for a wide range of wavelengths (ultraviolet/VIS/NIR/infrared/far-infrared/THz/sub-mm/radio) from any observatory, orbiter or lander, and also includes a noise calculator. To compute the noise, PSG takes into account the noise introduced by the source itself ($N_{\rm source}$), the background noise ($N_{\rm back}$), following a Poisson distribution with fluctuations depending on $\sqrt{N}$ with N the mean number of photons received[22], the noise of the detector ($N_{\rm D}$) and the noise introduced by the telescope ($N_{\rm optics}$), the total noise being then $N_{\rm total} = \sqrt{N_{\rm source} + N_{\rm back} + N_{\rm D} + N_{\rm optics}}$. This represents therefore a photon-limited situation where $N_{\rm source}$ will strongly dominate $N_{\rm total}$. For Earth-like atmospheres, spectra were obtained for each of the 98 Atmos photochemical simulations and an average spectrum was computed. For the 1- and 22-bar O_2 desiccated atmospheres, isothermal profiles from 200 to 600 K were set up with 100% O_2, ignoring photochemistry. To calculate the SNR and the number of transits needed for 3σ and 5σ detection, the resolving power has been optimized by adjusting the binning for each O_2 feature to maximize its SNR. SNR is calculated using the highest value in the band minus the nearest continuum value (this value therefore differs between the VIS (Rayleigh slope), NIR and MIR). The number of transits needed to achieve an $X\sigma$ detection is computed with the following equation:

$$N^{X\sigma}_{\rm transits} = N_{\rm i}(X/{\rm SNR_i})^2 \tag{3}$$

with $X\sigma$ the confidence level of value X and $N_{\rm i}$ the initial number of transits at which ${\rm SNR_i}$ is computed. If ${\rm SNR_i}$ is estimated from one transit then $N_{\rm i} = 1$ and equation (3) can be simplified as

$$N^{X\sigma}_{\rm transits} = (X/{\rm SNR_i})^2 \tag{4}$$

O_2–X CIA at 6.4 µm. This feature is associated with the fundamental band of O_2, and O_2 collisions with other partners (for example N_2, CO_2) can produce additional absorption at these wavelengths. This collision with other gases can be generally written as O_2–X, where X refers to the collision partner. Laboratory measurements[1,23] and atmospheric analysis using Sun occultations[3] have revealed that nitrogen, the major constituent of modern Earth's atmosphere at 78% by volume, produces an O_2–N_2 absorption feature of a similar intensity to O_2–O_2 in the 6.4-µm region. CO_2 can also produce an O_2–CO_2 feature at these wavelengths; this feature is weak for modern Earth-like CO_2 atmospheric abundances (approximately 400 ppm) but can be strong for exoplanets with CO_2-rich atmospheres[4]. O_2–X CIAs can also be produced with H_2O[24] as the collision partner due to the large electric dipole moment of H_2O, but no laboratory measurements exist for this feature.

Parameterization of the 6.4-µm feature. While the 6.4-µm region is known as the fundamental vibration–rotation band of O_2, only the O_2–O_2 CIA band is included in HITRAN[25]. Knowing that Earth's atmosphere is mostly composed of N_2 and that the O_2–N_2 CIAs have been shown to produce similar absorption to O_2–O_2[1,3,23], it is important to include it in our simulations. We have parameterized the O_2–N_2 CIA in PSG assuming the same absorption efficiency as for the O_2–O_2 CIA[3] (Supplementary Fig. 1). For the O_2–CO_2 CIA at 6.4 µm, we used experimental data from ref. [4] to include this feature in PSG.

Data availability

The data that support the plots within this paper and other findings of this study are available from the corresponding author on reasonable request.

Code availability

Atmos[8] is available on request from G.A. (giada.n.arney@nasa.gov); LMD-G[7] is available on request from M.T. (martin.turbet@lmd.jussieu.fr); PSG[6] is available at https://psg.gsfc.nasa.gov/

Received: 7 June 2019; Accepted: 15 November 2019;
Published online: 06 January 2020

References

1. Timofeyev, Y. & Tonkov, M. Effect of the induced oxygen absorption bond on the transformation of radiation in the 6 µm region. *lzv. Acad. Sci. USSR Atmos. Ocean. Phys.* **14**, 614–620 (1978).
2. Rinsland, C. P. et al. Stratospheric measurements of collision-induced absorption by molecular oxygen. *J. Geophys. Res. Oceans* **87**, 3119–3122 (1982).
3. Rinsland, C. P., Zander, R., Namkung, J. S., Farmer, C. B. & Norton, R. H. Stratospheric infrared continuum absorptions observed by the ATMOS instrument. *J. Geophys. Res. Atmos.* **94**, 16303–16322 (1989).
4. Baranov, Y. I., Lafferty, W. & Fraser, G. Infrared spectrum of the continuum and dimer absorption in the vicinity of the O_2 vibrational fundamental in O_2/CO_2 mixtures. *J. Mol. Spectrosc.* **228**, 432–440 (2004).
5. Luger, R. & Barnes, R. Extreme water loss and abiotic O_2 buildup on planets throughout the habitable zones of M dwarfs. *Astrobiology* **15**, 119–143 (2015).
6. Villanueva, G. L., Smith, M. D., Protopapa, S., Faggi, S. & Mandell, A. M. Planetary Spectrum Generator: an accurate online radiative transfer suite for atmospheres, comets, small bodies and exoplanets. *J. Quant. Spectrosc. Radiat. Transf.* **217**, 86–104 (2018).
7. Wordsworth, R. D. et al. Gliese 581d is the first discovered terrestrial-mass exoplanet in the habitable zone. *Astrophys. J. Lett.* **733**, L48 (2011).
8. Arney, G. et al. The pale orange dot: the spectrum and habitability of hazy Archean Earth. *Astrobiology* **16**, 873–899 (2016).
9. Lincowski, A. P. et al. Evolved climates and observational discriminants for the TRAPPIST-1 planetary system. *Astrophys. J.* **867**, 76 (2018).
10. Lustig-Yaeger, J., Meadows, V. S. & Lincowski, A. P. The detectability and characterization of the TRAPPIST-1 exoplanet atmospheres with JWST. *Astron. J.* **158**, 27 (2019).
11. Gillon, M. et al. Seven temperate terrestrial planets around the nearby ultracool dwarf star TRAPPIST-1. *Nature* **542**, 456–460 (2017).
12. Misra, A., Meadows, V., Claire, M. & Crisp, D. Using dimers to measure biosignatures and atmospheric pressure for terrestrial exoplanets. *Astrobiology* **14**, 67–86 (2014).
13. Wordsworth, R. & Pierrehumbert, R. Abiotic oxygen-dominated atmospheres on terrestrial habitable zone planets. *Astrophys. J,* **785**, L20 (2014).
14. Schwieterman, E. W. et al. Identifying planetary biosignature impostors: spectral features of CO and O_4 resulting from abiotic O_2/O_3 production. *Astrophys. J.* **819**, L13 (2016).
15. Meadows, V. S. Reflections on O_2 as a biosignature in exoplanetary atmospheres. *Astrobiology* **17**, 1022–1052 (2017).
16. Meadows, V. S. et al. Exoplanet biosignatures: understanding oxygen as a biosignature in the context of its environment. *Astrobiology* **18**, 630–662 (2018).
17. Des Marais, D. J. et al. Remote sensing of planetary properties and biosignatures on extrasolar terrestrial planets. *Astrobiology* **2**, 153–181 (2002).
18. Kasting, J. F., Whitmire, D. P. & Reynolds, R. T. Habitable zones around main sequence stars. *Icarus* **101**, 108–128 (1993).
19. Kopparapu, R. K. et al. Habitable zones around main-sequence stars: new estimates. *Astrophys. J.* **765**, 131 (2013).
20. Kopparapu, R. K. et al. Habitable zones around main-sequence stars: dependence on planetary mass. *Astrophys. J.* **787**, L29 (2014).

21. Grimm, S. L. et al. The nature of the TRAPPIST-1 exoplanets. *Astron. Astrophys.* **613**, A68 (2018).
22. Zmuidzinas, J. Thermal noise and correlations in photon detection. *Appl. Opt.* **42**, 4989–5008 (2003).
23. Thibault, F. et al. Infrared collision-induced absorption by O_2 near 6.4 μm for atmospheric applications: measurements and empirical modeling. *Appl. Opt.* **36**, 563–567 (1997).
24. Hopfner, M., Milz, M., Buehler, S., Orphal, J. & Stiller, G. The natural greenhouse effect of atmospheric oxygen (O_2) and nitrogen (N_2). *Geophys. Res. Lett.* **39**, L10706 (2012).
25. Gordon, I. et al. The HITRAN2016 molecular spectroscopic database. *J. Quant. Spectrosc. Radiat. Transf.* **203**, 3–69 (2017).

Acknowledgements

T.J.F., G.L.V., G.A., R.K.K., A.M. and S.D.D.-G. acknowledge support from the GSFC Sellers Exoplanet Environments Collaboration (SEEC), which is funded in part by the NASA Planetary Science Divisions Internal Scientist Funding Model. This project has received funding from the European Union's Horizon 2020 research and innovation programme under the Marie Sklodowska-Curie Grant Agreement 832738/ESCAPE. This work was also supported by the NASA Astrobiology Institute Alternative Earths team under Cooperative Agreement NNA15BB03A and the NExSS Virtual Planetary Laboratory under NASA grant 80NSSC18K0829. E.W.S. is additionally grateful for support from the NASA Postdoctoral Program, administered by the Universities Space Research Association. We thank H. Tran for useful discussions related to O_2–X CIAs.

Author contributions

T.J.F. led the photochemistry and transmission spectroscopy simulations. G.L.V., E.W.S. and M.T. derived parameterizations of the O_2–N_2 and O_2–CO_2 CIA bands. T.J.F. and G.A. wrote most of the manuscript. All the authors contributed to the discussions and to the writing of the manuscript.

Competing interests

The authors declare no competing interests.

Additional information

Supplementary information is available for this paper at https://doi.org/10.1038/s41550-019-0977-7.

Correspondence and requests for materials should be addressed to T.J.F.

Peer review information *Nature Astronomy* thanks Sergei Yurchenko and the other, anonymous, reviewer(s) for their contribution to the peer review of this work.

Reprints and permissions information is available at www.nature.com/reprints.

Publisher's note Springer Nature remains neutral with regard to jurisdictional claims in published maps and institutional affiliations.